

# Can Nonpremixed Stretched Flames Become Infinitely Thin?

Viswanath R. Katta<sup>1</sup>, William M. Roquemore<sup>2</sup>, James R. Gord<sup>2</sup>

<sup>1</sup>Innovative Scientific Solutions Inc,  
2766 Indian Ripple Road, Dayton, OH 45440, USA

<sup>2</sup>Propulsion Directorate, Air Force Research Laboratory,  
Wright Patterson Air Force Base, OH 45433, USA

## 1 Introduction

Laminar flamelet is an asymptotic concept introduced by Peters [1] for describing turbulent flames. If the relevant chemical time scales are short compared to the convection and diffusion time scales, according to flamelet concept, combustion takes place within asymptotically thin layers embedded in the turbulent flow. In other words, laminar flamelet concept allows turbulent fluctuations in a reaction layer to be treated as variations to the flame structure rather than deviations to the structure itself. The usefulness of laminar flamelet concept in modeling turbulent flames comes from the assumption that the local instantaneous composition and temperature of the mixture in a nonpremixed system could be modeled as being the same as those in a stretched laminar flame [2]. The mixture fraction and scalar dissipation rate are commonly used in linking the turbulent flame structure to that of the laminar flame. At a critical value of scalar dissipation rate laminar nonpremixed flame extinguishes due to large mixture fraction gradients. The reaction zone in physical space under such critical conditions becomes so narrow that diffusive heat loss will lead to quenching. This scalar-dissipation-rate analogy has been used in flamelet theories in modeling extinction and ignition phenomena in turbulent flames. Flamelet theories have been successfully applied to the modeling of various nonpremixed flame systems [3].

A necessary condition for the flamelet concepts to be applied is that the reaction zone must be thinner than the smallest scales of the turbulence, which is Kolmogorov length scale. Performing asymptotic expansion for high Damkohler numbers for hydrogen flames, Bilger [4] derived an expression for reaction rate and argued that flamelets are not asymptotically thin due to the influence of reverse reactions; which means that the reaction zones must be broadened due to chemical equilibrium. Even though, the regular asymptotic analysis and the non-reacting experimental data used by Bilger [4] are not ideal for judging the validity of the flamelet theories, they certainly raised important issues about the applicability of the flamelet theories to the turbulent-combustion process. It has been widely recognized that highly resolved measurements and numerical simulations are needed for addressing the existence of laminar flamelets in turbulent-flow environment [5].

Recent numerical simulations of micro-vortex/flame interactions [6] suggested that vortices that are smaller than a millimeter in size cannot stretch a laminar nonpremixed flame. Instead, they destroy the flame structure during the interaction process. Even though these findings pose questions on the validity of the laminar flamelet concept, they could not disapprove the existence of infinitely thin reaction layers. A weak hydrogen-air nonpremixed flame is aerodynamically stretched in the present study for identifying the limits, if any, on the reaction layer thickness. The effect of chemical equilibrium on reaction layer thickness is also investigated.

## 2 Mathematical Model

A time-dependent axisymmetric model known as UNICORN (UNsteady Ignition and COmbustion using ReactionNs) [7] is used for the simulations of steady flames associated with an opposed-jet burner. This model solves the Navier-Stokes and species- and energy-conservation equations written in the cylindrical-coordinate ( $z$ -

r) system. A detailed-chemical-kinetics model is employed for describing the hydrogen-air combustion process. This model consists of 13 species--namely,  $H_2$ ,  $O_2$ ,  $H$ ,  $O$ ,  $OH$ ,  $H_2O$ ,  $HO_2$ ,  $H_2O_2$ ,  $N$ ,  $NO$ ,  $NO_2$ ,  $N_2O$ , and  $N_2$ --and 74 elementary reactions (37 forward and 37 backward) among the constituent species. The rate constants for this  $H_2$ - $O_2$ - $N_2$  reaction system were obtained from Ref. [8].

Temperature- and species-dependent property calculations are incorporated in the model. The governing equations are integrated on a nonuniform staggered-grid system. An orthogonal grid having rapidly expanding cell sizes in both the axial and the radial directions is employed. The finite-difference forms of the momentum equations are obtained using an implicit QUICKEST scheme [9], and those of the species and energy equations are obtained using a hybrid scheme of upwind and central differencing. At every time step, the pressure field is calculated by solving the pressure Poisson equations simultaneously and utilizing the LU (Lower and Upper diagonal) matrix-decomposition technique. UNICORN has been validated previously by simulating various steady and unsteady opposed and coflow jet nonpremixed flames [7,10].

The opposed-jet-flow burner, shown in Fig. 1, consists of two concentric nozzle systems. Fuel (a mixture of hydrogen and nitrogen) is issued from the top nozzle ( $d_0 = 20$  mm) while air is issued from the bottom. Low speed nitrogen shroud flows ( $D_0 = 30$  mm) are used for both the fuel and air jets. The top and bottom nozzles are separated by 20 mm. A flat nonpremixed flame is formed between the fuel and air jets in the neighborhood of the stagnation plane. The weak flame established with hydrogen-to-nitrogen ratio of 0.38 is aerodynamically stretched by increasing the fuel and air jet velocities simultaneously. The  $z$ - $r$  coordinate system and a typical computed flame are shown in Fig. 1. Note, only one half of the flame shown in this figure is calculated. A non-uniform  $801 \times 51$  mesh system distributed over a physical domain of  $20 \times 20$  mm in the region between the upper and lower nozzles is used. An uniform mesh spacing of 0.02 mm in the axial ( $z$ ) direction across the flame width and a rapidly increasing grid spacing in the radial ( $r$ ) direction starting from 0.02 mm spacing at the axis of symmetry are achieved with this grid system.

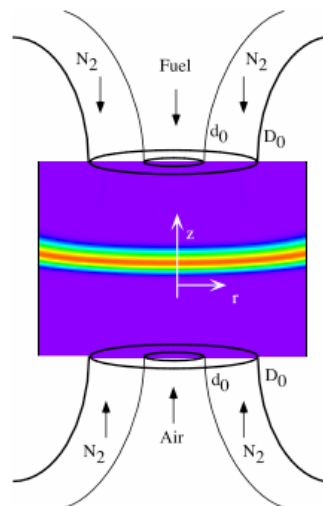


Fig. 1. Schematic diagram of the opposed-jet-flow burner modeled.

### 3 Results and Discussion

The steady-state flame shown in Fig. 1 represents a weakly stretched laminar flame obtained with fuel and air jet velocities of 0.4 and 0.3 m/s, respectively. As the velocities of the fuel and air jets increased, flame becomes thinner and its temperature decreases. Flame extinguishes for a critical set of velocities. Variations in flame (peak) temperature and peak heat-release rate along the centerline with respect to scalar dissipation rate at stoichiometry ( $\chi_{st}$ ) are shown in Fig. 2 for velocities ranging from 0.3 m/s through 21 m/s. Scalar dissipation rate ( $\chi$ ) is calculated from mixture-fraction formulation of Bilger [4] and using  $1 \text{ m}^2/\text{s}$  for diffusion coefficient [11]. Results are labeled with “normal kinetics” while the open circles represent the values of the maximum-stretched flame. Further stretching of the flame resulted in extinguishment. The opposed-jet flame shown in Fig. 1 extinguished when the temperature dropped to 1140 K at which the scalar dissipation rate was  $1.12 \text{ s}^{-1}$ . To understand the role of chemical equilibrium on flame structure, calculations for the opposed-jet flame are repeated after increasing or decreasing the rates of the chemical reactions. Three sets of data with modified reaction rates are shown in Fig. 2. Results obtained after reducing the rates of the 37 forward reactions by half are shown with dash-dot lines, those obtained after doubling the rates of the forward reactions are shown in broken lines, and those obtained after doubling the rates of both the forward and reverse reactions are shown in thin lines. Changes in reaction rates affected not only the maximum stretch rate that can be applied on this flame but also the temperature at which extinction takes place. In general, temperature and heat release rates at extinction are higher with faster reactions. At a given scalar dissipation rate ( $\chi_{st}$ ) temperature and heat release rate of the flame increase with the reactivity of the system and such increase is more pronounced at higher  $\chi_{st}$ .

This behavior can be explained from the chemical-nonequilibrium state of the flame. Increase in reaction rates enhances reactivity in the flame zone and, thereby, shifts the flame more into equilibrium.

Flame thickness estimated based on the full width of the temperature profile is shown in Fig. 3 for different  $\chi_{st}$  values and for different chemical kinetics. Thicknesses of the flame at the time of extinction are marked with open circles. As the stretch rate increased on the steady opposed-jet flame, its thickness decreased as suggested by the laminar flamelet theory. However, contrary to the assumption that stretched flames become infinitely thin prior to extinction, flame thicknesses at extinction obtained with normal, reduced and enhanced kinetics are all within the range of 1 and 2 mm. More interestingly, the thickness Vs  $\chi_{st}$  plot suggests that flame thickness is asymptotically approaching a finite value ( $\sim 1$  mm).

One could argue that temperature profile may not necessarily represent the reaction zone thickness as the it will be influenced by the thermal and molecular diffusive transport. Typically, intermediate radical species such as OH, O, and H that have short lifespan are confined to reaction zones. Variations of flame thicknesses obtained from the full width of OH and O radical distributions are shown in Figs. 4 and 5, respectively. For a given scalar dissipation rate, reaction zone thicknesses obtained from OH and O radical distributions are about one half of that obtained from temperature. Figs. 4 and 5 suggest that the radical-based reaction-zone thicknesses are also asymptotically approaching a finite value as the scalar dissipation rate on the flame is increased. It is important to note that even the smallest thickness of 0.5 mm represents a radical profile that has been resolved with a large number (25) of grid points, and hence, the asymptotic thicknesses shown in Figs. 3-5 are not limited by the grid distribution.

An examination of Figs. 4 and 5 further reveals that when the forward reaction rates ( $k_f$ ) are reduced by half, the thickness of the reaction zone has increased for the similarly stretched flames (equal scalar dissipation rates). When the forward reaction rates are increased by 100% the reaction zone thickness decreased for the similarly stretched flames. On the other hand, when the reverse reaction rates ( $k_b$ ) are also doubled the reaction zone thickness did not change much. This suggests that the flames calculated using twice the normal reaction rates are in chemical equilibrium and any further increase in reaction rates doesn't decrease the reaction-zone thickness. Which means flames are broadened (from infinitely thin reaction zone) not due to finite-rate chemistry, but due to equilibrium condition.

Calculations made with different reaction rates suggest that a minimum reaction zone thickness exists for flames that are aerodynamically stretched. For the hydrogen flame considered in this study, the minimum reaction zone thickness is in the range 0.5-1.0 mm, depending on the radical species used for obtaining the thickness. Consequently, flamelet theory cannot be applied to hydrogen-air nonpremixed flames for turbulent fluctuation length scales that are smaller than 0.5 mm. This was also evident in our previous studies [6] on vortex/flame interactions in which vortices smaller than 0.5 mm in diameter failed in stretching the flame.

## 4 Conclusions

A numerical study has been performed for determining the minimum possible thickness for a nonpremixed hydrogen-air flame. The flat flame formed between the counter flowing fuel and air jets is stretched through increasing jet velocities. A time-dependent model, known as UNICORN, that incorporates 13 species and 74 reactions among the constituent species has been used for the simulation of opposed-jet hydrogen-air nonpremixed flame. Numerical experiments were performed through changing the reaction rates. It is found that a nonpremixed flame can only be stretched to a minimum thickness prior to its extinction. Contrary to the flamelet description for laminar stretched flames, the reaction zone thickness for a hydrogen-air nonpremixed flame can asymptotically reach a value in the range 0.5-1.0 mm, depending on the radical species used for measuring the thickness. This finding has an important bearing on turbulence modeling based on flamelet theory.

## References

- [1] N. Peters, *Proc. Combust. Inst.* 21 (1986) 1231-1256.
- [2] N. Peters, Length Scales in Laminar and Turbulent Flames, in Numerical Approaches to Combustion Modeling, (Eds. E. S. Oran and J. P. Boris), Progress in Astronautics and aeronautics, Vol. 135, 1991, Washington, D. C.

- [3] S. K. Liew, K. N. C. Bray, J. B. Moss, *Comb. Flame*, 56 (1984) 199-213.
- [4] R. W. Bilger, *Proc. Combust. Inst.* 22 (1988) 475-488.
- [5] N. Peters, *Prog. Astronautics Aeronautics* 135 (1991) 155-182.
- [6] V. R. Katta, T. R. Meyer, J. R. Gord, and W. M. Roquemore, Micro-Vortex/Flame interactions and Their Implication in Turbulent-Flame Modeling, 2005 Technical Meeting of the eastern States section of the Combustio Institute, Orlando, FL, Nov. 13-15, 2005.
- [7] W. M. Roquemore and V. R. Katta, *J. Visualization* 2 (2000) 257.
- [8] M. Frenklach, H. Wang, M. Goldenberg, G. P. Smith, D. M. Golden, C. T. Bowman, R. K. Hanson, W. C. Gardiner, V. Lissianski, Gas Research Institute Technical Report No. GRI-95/0058 (Gas Research Institute, Chicago), November 1, 1995.
- [9] V. R. Katta, L. P. Goss, W. M. Roquemore, *AIAA J.* 32 (1994) 84.
- [10] V. R. Katta and W. M. Roquemore, *AIAA J.* 36 (1998) 2044.
- [11] V. R. Katta, T. R. Meyer, M. S. Brown, J. R. Gord, and W. M. Roquemore, *Combust. Flame* 137 (2004) 198-221.

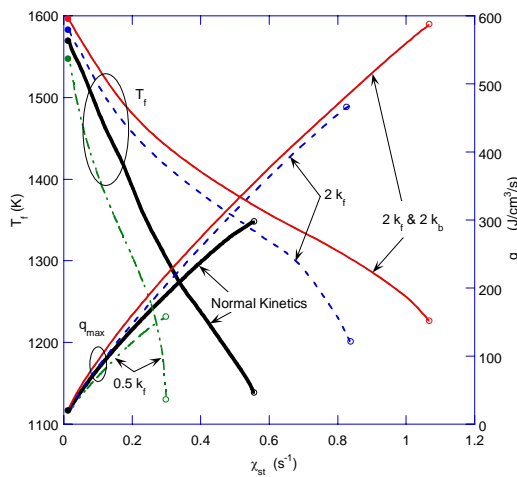


Fig. 2. Response of a steady state flame to aerodynamic stretch for different (fast vs slow) chemical kinetics.

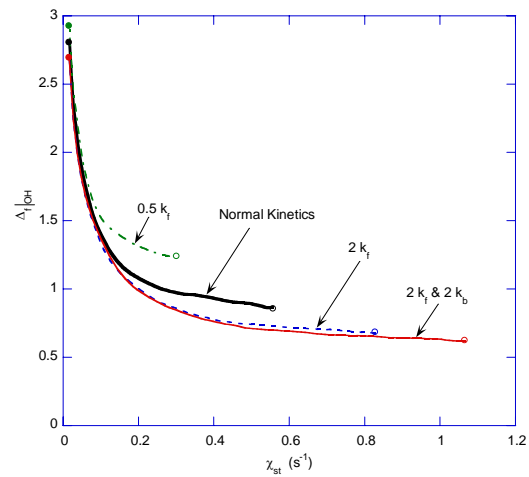


Fig. 4. Thickness (based on OH concentration) of a steady state flame at different stretch rates.

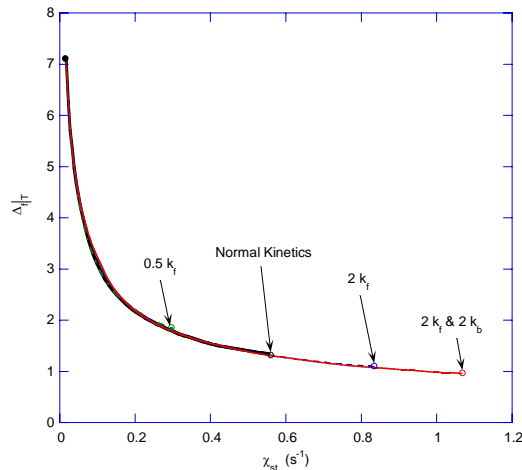


Fig. 3. Thickness (based on Temperature) of a steady state flame at different stretch rates and with different (fast vs slow) chemical kinetics.

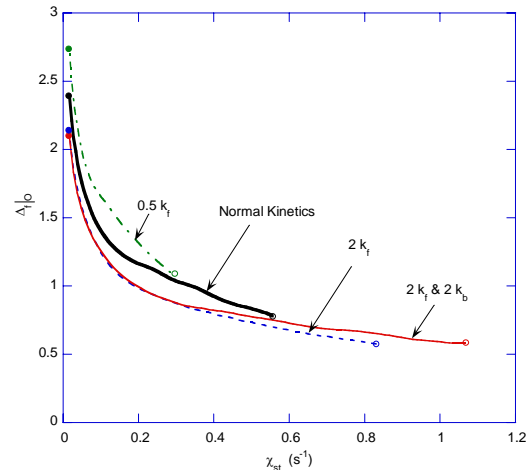


Fig. 5. Thickness (based on O concentration) of a steady state flame at different stretch rates.